Available online at www.sciencedirect.com

ScienceDirect

Procedia Engineering 67 (2013) 397 – 403

Procedia Engineering

www.elsevier.com/locate/procedia

7th Asian-Pacific Conference on Aerospace Technology and Science, 7th APCATS 2013

Viscoelastic Properties of Foam Under Hydrostatic Pressure and Uniaxial Compression

Y. C. Wang[a,*], C. C. Ko[a], Y. H. Huang[a]

[a]*Department of Civil Engineering, National Cheng Kung University, Tainan 70101, Taiwan*

Abstract

Foam is a lightweight material suitable for aerospace applications for load bearing structures or noise reduction media. The microstructure of the foam, which is constructed with cell ribs, allows its unique mechanical properties. In this work, commercial polyurethane foams with a pore size on the order of a few hundred microns were subjected to quasi-static hydrostatic and uniaxial compression at low strain rates, as well as dynamic sinusoidal loading for studying their loss tangent and storage modulus. The identified incremental negative modulus depends on deformation modes, and it is been shown hydrostatic compression may trigger the negative bulk modulus mode, while uniaxial compression may not. The use of negative modulus in composite materials may lead to extreme high damping and high stiffness materials. Furthermore, by finite element calculations on a dodecahedral unit cell with different elastic constant, it is found that high elastic constant of the cell ribs may give rise to larger negative stiffness effects, when the cell in under hydrostatic compression.

Keywords: Viscoelastic properties, foam, negative stiffness, hydrostatic pressure, uniaxial compression

Nomenclature

e	Exponential function
E(t)	Relaxation modulus
E_0	Initial relaxation modulus
E_∞	Fully relaxed modulus
J(t)	Creep compliance
J_0	Initial creep compliance
t	Time
Greek symbols	

* Corresponding author. Tel.: +886-6-2757575-63140; fax: +886-6-2358542.
E-mail address: yunche@mail.ncku.edu.tw

doi:10.1016/j.proeng.2013.12.039

τ	Integration variable
τ_c	Time constant for creep
τ_r	Time constant for relaxation

1. Introduction

Recently, it has been shown that under quasi-static compression polymeric foam may exhibit incremental negative bulk modulus [1]. The negative modulus may be adopted to create novel composites to exhibit extreme high damping materials [2], or extreme high stiffness materials [3]. Although the bulking of single unit cell of foam has long been recognized [4], it is generally considered for the explanation of stress-strain plateau mechanism when foam under uniaxial compression. The stress-strain plateau in foam before densification is due to organized micro-buckling of the foam cells, but not simultaneously. However, under hydrostatic compression, simultaneous micro-buckling may occur, and hence macroscopic negative bulk modulus is obtained. In addition to the rib buckling mechanism, the time-dependent properties of the foam are crucial in understanding the mechanical behavior of the foam. Computational efforts to study mechanical properties of foam are vast. Most of the studies adopted hyperelastic model to consider the effects of nonlinear elasticity from large deformation [5, 6]. To this date, computer simulation of large foam sample still poses difficulties in terms of large deformation, material nonlinearity and material time dependence.

In this work, polymeric foam is studied experimentally. Both hydrostatic and uniaxial compression tests were adopted to cross-check experimental data from different deformation modes. In addition, computer simulation was performed to identify the origin of incremental negative bulk modulus.

2. Sample preparation

For hydrostatic compression tests, foam specimens were sectioned from 3M company (Minnesota, USA) polyurethane foam, named as Foam 1 specimen. For uniaxial compression tests, a similar foam specimen with a different cell size were adopted, named as Foam 2 specimen. Both of the foam specimens were open celled with an estimated pore size on the order of a few hundred microns. The cell size of Foam 1 specimen was greater than that of Foam 2 specimen. For both hydrostatic and uniaxial testing, the foam specimens had a volume of approximately 20 cm^3. And, Their shape of the pores appeared to be tetradecahedrons with some distortion, but in the finite element modeling a dodecahedron is adopted.

3. Experimental

The uniaxial testing was performed with a 25 kN servo-hydraulic MTS load frame, as shown in Figure 1 (a), with a blue foam specimen being compressed. The two platens were in contact with the foam samples, and the top platen was attached to the actuator of the load frame. Loads and displacements are directly measured by the MTS machine. Since the foam is relative low stiffness, machine compliance errors may be ignored.

As for the hydrostatic tests, shown in Figure 1 (b), a volumetric compression chamber was built which could be held in the same MTS load frame. The test chamber was a 20 cm long acrylic tube with a 13 mm inner diameter. When installed in the MTS load frame, the bottom plate is rigidly held in the bottom grip, the top grip holds the piston. The working fluid was tap water at ambient temperature. To provide surface constraint, and hence volume compression, foam specimens were sealed inside thin rubber membranes with electrical tape. An air escape tube, with access through the bottom plate, was also included. Water pressure was measured using an Impress DMP331 (Berkshire, UK) pressure sensor which uses a stainless steel membrane for pressure measurement. Linear displacements of the piston were measured using the MTS's actuator.

(a) 

(b) 

Fig.1. Photos of experimental components. (a) Foam under uniaxial compression, and (b) the hydrostatic testing chamber.

4. Numerical

In order to model the three-dimensional mechanical behavior of the foam unit cell, the finite element solver, COMSOL Multiphysics [7], was adopted for numerical calculations. The open-cell foam is modeled as a dodecahedral polyhedron, and its ribs are assumed to be the elastic truss element. Only hydrostatic compression is modeled to disclose the negative stiffness properties of the foam unit cell. In the calculations, both of the geometrical and material linearity are assumed. Detailed information about the finite element model and parameters is discussed in the next section along with the results of calculations in Figure 5.

5. Results and Discussions

Negative incremental stiffness was observed in the quasi-static tests, as shown in Figure 2 (a), around 14% volume change, when the Foam 1 specimen is under hydrostatic compression. The initial slope shows the bulk modulus of the foam was about 22.3 kPa, and increased to 46.3 kPa before exhibiting incremental negative bulk modulus. This increase may be due to cell shape change before micro-buckling occurs. The magnitude of the incremental negative bulk modulus is about B = 30.1 kPa. The foam sample collapsed at about 20% volume change, as shown by a steep drop in the load-displacement curve.

Non-monotonic load-displacement curves obtained from buckled tubes and single foam cells subjected to displacement controlled uniaxial compression are due to negative stiffness of the structural elements in the post-buckled regime. In the continuum limit, non-monotonic stress-strain curves obtained for elastomeric foams under volume controlled hydrostatic compression indicate negative incremental bulk moduli, which arises form a collective behavior of each single cell. In this case, negative bulk modulus of the foam arise from cell rib buckling stabilized from collapse by the volumetric constraint of neighboring cells.

Figure 2 (b) shows the results of the uniaxial compression tests on the Foam 2 specimen. The tests were performed under the displacement control, and the tests stopped at the maximum engineering strain of about 0.38. Since polymeric foam is quite ductile, no fracture damages were observed after the maximum displacement loading. In order to avoid material memory effects, it was waited at least an hour before each test. The uniaxial compression tests were performed to obtain Young's modulus of the foam, as well as its creep properties. No

negative incremental Young's modulus was observed, as shown in Figure 2 (b). It is known that under uniaxial compression, the foam ribs may undergo micro-buckling such as a stress-strain plateau may be observed. In the tested strain rates, the plateau behavior is not significant. Since the sample height is about 50 mm, the displacement rates can be converted to strain rates by a factor of 0.02. It can be seen that the measured Young's modulus depends on the displacement loading rates. Higher loading rates give rise to larger elastic constants in the linear regime. At large strains, strain rates appear no in relation to the tangential modulus, maybe due to complex interactions between micro-buckling of the ribs and contact between the ribs during densification.

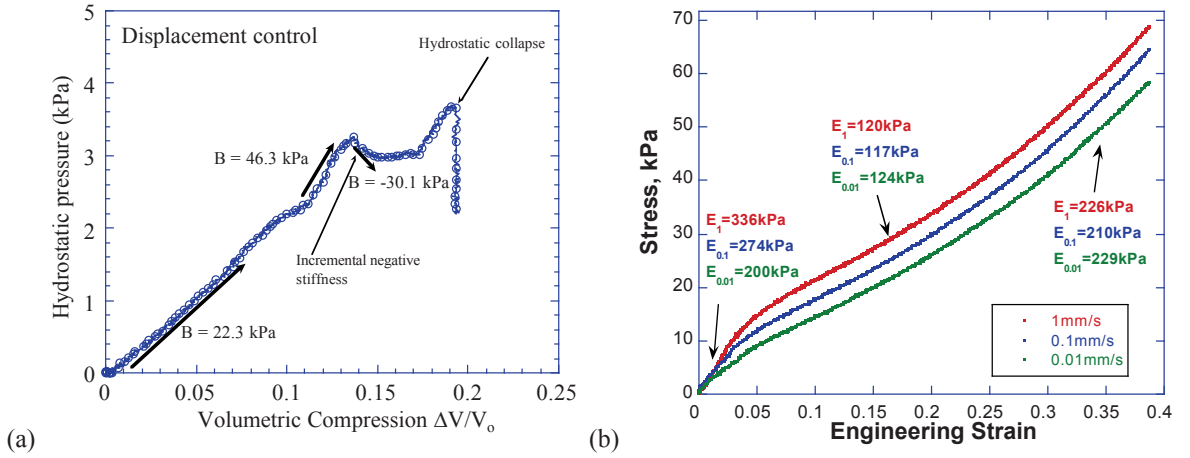

Fig. 2. Quasi-static testing results. (a) foam under hydrostatic pressure, and (b) foam under uniaxial compression under three displacement loading rates.

Creep and stress relaxation data are shown in Figure 3 (a) and (b), respectively. Our time-dependent tests disclosed power law behavior for uniaxial compression relaxation. It can be seen that the foam material exhibits strong time dependence, and single exponential function with a time constant τ_c may be adopted to model the creep compliance J(t) from initial compliance J_0.

$$J(t) = J_0(1 - e^{-t/\tau_c}) \quad (1)$$

Simialrly, the relaxation modulus E(t) can also be modeled by a single exponential function with a time constant τ_r.

$$E(t) = (E_0 - E_\infty)e^{-t/\tau_r} \quad (2)$$

The initial and fully relaxed modulus are denoted as E_0 and E_∞, respectively. Since both functions describe the same material but under different loading conditions, a linear viscoelastic material would satisfy Equation (3), as follows.

$$\int_0^t J(t-\tau)E(\tau)d\tau = t \quad (3)$$

If the foam is a linear viscoelastic material, the measured time-dependent modulus would obey the above equation, which will be verified in our future studies. Furthermore, the single exponential form for the modulus implies the foam material can be modeled as the standard linear solid. In addition, the strain rate effects in the quasi-static tests are a consequence of the time dependence of relaxation modulus. It is noted that under hydrostatic compression the bulk relaxation may be obtained to directly test the isotropy of the foam along with uniaxial data.

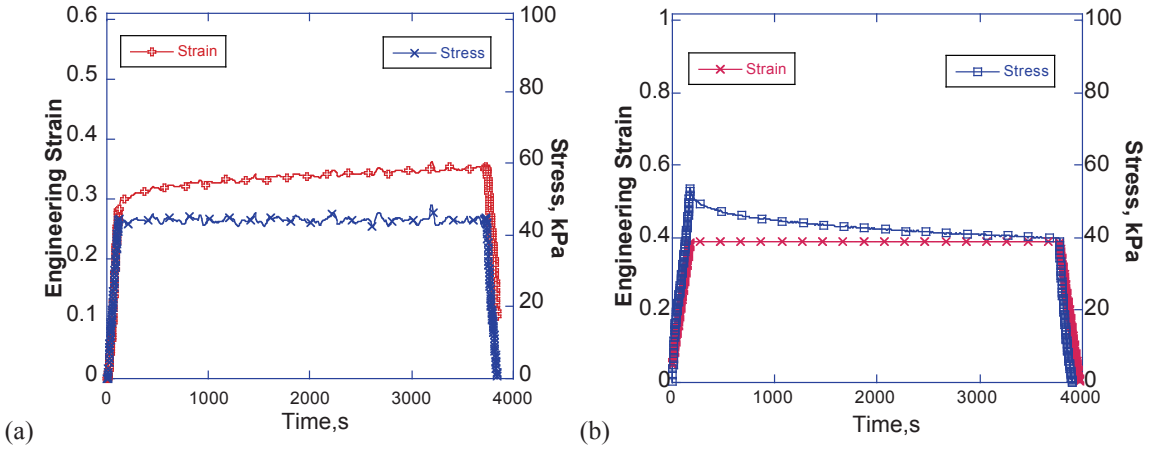

Fig. 3. Time-dependent experimental data. (a) Creep and (b) stress relaxation from uniaxial tests.

Dynamic testing data under sinusoidal displacement control at low frequency about 1 Hz are shown in Figure 4 (a) and (b) for the hydrostatic and uniaxial compression, respectively. The loss tangent, which is proportional to the size of the ellipse of the Lissajous curve, is larger in the hydrostatic case due to the friction between the actuator and hydrostatic chamber. From the uniaxial tests the tangent delta of the foam is about 0.16. Furthermore, it can be seen that a significant ratcheting effect, i.e. dynamic process affected by creep, are observed. Under hydrostatic loading, this ratcheting effect is not significant since creep is controlled by the deviatoric stresses.

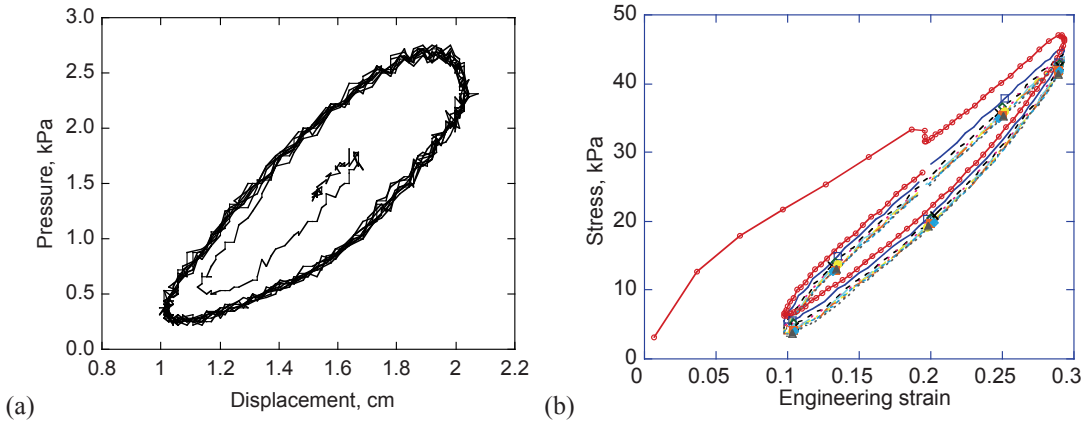

Fig. 4. Dynamic test results under sinusoidal displacement loading at 1 Hz for (a) Hydrostatic compression and (b) uniaxial compression.

From the creep, stress relaxation and dynamic tests, we obtained data from hydrostatic and uniaxial loading conditions to correlate the three-dimensional isotropic viscoelastic properties of the foam. It is found that the foam satisfies the linear viscoelastic model, and negative bulk modulus may only obtain from hydrostatic compression, not from uniaxial loading. The rationale is uniaxial loading creates micro-buckling cascade events of cell ribs, while hydrostatic loading triggers a simultaneous micro-buckling event.

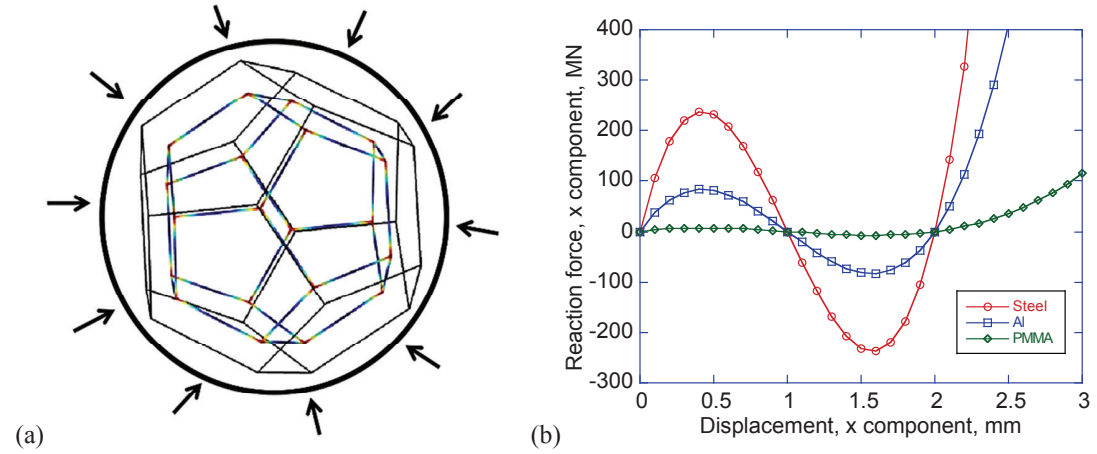

Fig. 5. Finite element calculation of the three-dimensional dodecahedron unit cell under hydrostatic compression. (a) Deformation of the unit cell (color indicates stress; red maximum and blue minimum) with schematic loading configuration, and (b) the load-displacement curve.

To further demonstrate negative stiffness, Figure 5 shows the numerical studies of the negative bulk stiffness properties of the foam cell under hydrostatic compression. Only elasticity is involved in this modeling. Three different materials were considered, namely polymethalmethacrylate (PMMA), aluminum and steel with the Young's modulus of 3 GPa, 70 GPa and 200 GPa, respectively. The Poisson's ratio for the three materials was assumed to be 0.3. The edge length of a cell rib is about 1.23 mm. In Figure 5 (a), the dodecahedron unit cell model is shown, as well as its typical deformed configurations (colored inside). The color on the deformed shape indicates the magnitude of the stress. The outer circle with illustrated arrows pointing at the center of the foam indicates the displacement loading configuration. In actual calculations, the displacements of the vertices are controlled to move toward the center of the foam, to mimic the hydrostatic compression. To quantify the force-displacement relationship of the foam, we selected a vertex of the dodecahedron, and recorded the displacement and total reaction force exerting on the vertex. In Figure 5 (b), the load-displacements of the three materials are shown at different level of displacement compression under the hydrostatic assumption, since all calculations done here are time independent. It can be seen that higher Young's modulus give rise stronger negative slope in the post-buckling regime.

6. Conclusion

Polymeric foam was experimentally studied for its mechanical behavior under hydrostatic and uniaxial compression. Under hydrostatic testing, the Foam 1 specimen showed a bulk modulus of 22.3 kPa at the low volume reduction rate of 0.005 per second. Under uniaxial testing, the Foam 2 specimen exhibited as a linear viscoelastic solid with a Young's modulus about 200 kPa at a low strain rate, and loss tangent of 0.17 at 1 Hz.

Negative bulk modulus may only be obtained through hydrostatic compression, and the strength of the negativity depends on the modulus of the solid phase of the foam.

Acknowledgements

This research work was supported by the National Science Council of the Republic of China under Grant NSC 101-2221-E-006 -206.

References

[1] Deal, B., Grove, A., 1965. General Relationship for the Thermal Oxidation of Silicon, Journal of Applied Physics 36, p. 3770.
[2] Fachinger, J., 2006. Behavior of HTR Fuel Elements in Aquatic Phases of Repository Host Rock Formations. Nuclear Engineering & Design 236, p. 54.
[3] Quintiere, James G., 2006. Fundamentals of Fire Phenomena, John Wiley & Sons. Ltd, Chichester, U. K.
[4] Clark, T., Woodley, R., De Halas, D., 1962. Gas-Graphite Systems, in "Nuclear Graphite" R. Nightingale, Editor. Academic Press, New York, p. 387.
[5] Samochine, D., Boyce, K., Shields, J., 2005. "Investigation into staff behaviour in unannounced evacuations of retail stores - Implications for training and fire safety engineering," Fire Safety Science - Proceedings of the 8th International Symposium, International Association for Fire Safety Science, pp. 519-530.
[6] Fachinger, J., den Exter, M., Grambow, B., Holgerson, S., Landesmann, C., Titov, M., Podruhzina, T., 2004. "Behavior of spent HTR fuel elements in aquatic phases of repository host rock formations," 2nd International Topical Meeting on High Temperature Reactor Technology. Beijing, China, paper #B08.
[7] Deep-Burn Project: Annual Report for 2009, Idaho National Laboratory, Sept. 2009.